Transcriptomic Analysis Reveals the Key Role of Histone Deacetylation-mediated Phytohormones Interaction in Fiber Initiation of Cotton

Zhenzhen Wei (wzz19920315@163.com)
Zhengzhou University
Yonghui Li
Chinese Academy of Agricultural Sciences
Faiza Ali
Chinese Academy of Agricultural Sciences
Ye Wang
Chinese Academy of Agricultural Sciences
Jisheng Liu
Chinese Academy of Agricultural Sciences
Zuoren Yang
Chinese Academy of Agricultural Sciences
Fuguang Li
Chinese Academy of Agricultural Sciences
Zhi Wang
Zhengzhou University

Research Article

Keywords: Fiber initiation, Histone deacetylation, HDAC inhibitor, TSA, Phytohormones

Posted Date: December 22nd, 2021

DOI: https://doi.org/10.21203/rs.3.rs-1138074/v1

Transcriptomic analysis reveals the key role of histone deacetylation-mediated phytohormones interaction in fiber initiation of cotton

Zhenzhen Wei[a, #], Yonghui Li[a, #], Faiza Ali[a], Ye Wang[b], Jisheng Liu[a, b], Zuoren Yang[a, b], Fuguang Li[a, b]*, Zhi Wang[a, b]*

[a] Zhengzhou Research Base, State Key Laboratory of Cotton Biology, Zhengzhou University, Zhengzhou, 450001, China;

[b] State Key Laboratory of Cotton Biology, Institute of Cotton Research, Chinese Academy of Agricultural Sciences, Anyang, 455000, China

#, the authors contributed to this work equally

*, Correspondence:

Fuguang Li: aylifug@caas.cn

Zhi Wang: wangzhi01@caas.cn

Abstract:

Background: Histone deacetylation is one of the most important epigenetic modifications and plays diverse roles in plant development. However, the detailed functions and mechanisms of histone deacetylation in fiber development of cotton are still unclear. HDAC inhibitors (HDACi) have been used commonly to study the molecular mechanism underlying histone deacetylation or to facilitate disease therapy in humans through hindering the histone deacetylase catalytic activity. Trichostatin A (TSA) - the most widely used HDACi has been used to determine the role of histone

deacetylation on different developmental stages of plants.

Results: Here, exogenous TSA was applied in the fiber initiation and elongation in vitro, and the results demonstrated the crucial role of histone deacetylation in fiber initiation regulation. Therefore, we made a transcriptomic analysis to reveal the underlying mechanisms. Through RNA-Seq analysis, the differentially expressed genes were mostly enriched in plant hormone signal transduction, phenylpropanoid biosynthesis, photosynthesis, and carbon metabolism pathways, suggesting the potential role of phytohormone, phenylpropanoid metabolism, and energy metabolism downstream of histone deacetylation in fiber initiation. The phytohormone signal transduction pathways harbor the most differentially expressed genes. Deeper studies showed that some genes promoting auxin, Gibberellic Acid (GA), and Salicylic Acid (SA) signaling were down-regulated, while some genes facilitating Abscisic Acid (ABA) and inhibiting Jasmonic Acid (JA) singling were up-regulated after the TSA treatments.

Conclusions: Collectively, we established a model, in which histone deacetylation can regulate some key genes involved in different phytohormone pathways, consequently, promoting the auxin, GA, JA and SA signaling, whereas, repressing the ABA signaling to improve the fiber cell initiation; besides that the genes associated with energy metabolism, phenylpropanoid, and glutathione metabolism were also involved in. The above results provided novel clues to illuminate the underlying mechanisms of epigenetic modifications as well as interactions of different phytohormones in fiber cell differentiation, which is also very valuable for molecular

breeding of higher quality cotton.

Keywords: Fiber initiation, Histone deacetylation, HDAC inhibitor, TSA, Phytohormones

Backgroud

Histone acetylation functions as one type of the most important chromatin modifications in eukaryotes, which generally is mediated by the opposite functions of histone acetyltransferases (HATs) and histone deacetylases (HDACs) to sustain the balance of lysine acetylation for regulation of gene expression in the context (Ref). A lot of HDAC genes have been identified and characterized from animals, fungi, and plants to involve diverse developmental stages or stress tolerances [1-8]. Up to now, HDACs were classified into three subfamilies in eukaryotes. The first is most closely related to the yeast RPD3, and the second is related to yeast HDA1 [9]. Moreover, the third subfamily of HDACs (HD2) is unrelated to yeast RPD3 and unique in plants [10-13]. HDACs generally function as a part of multiprotein complexes consisting of transcriptional repressors, scaffold proteins, and a variety of cofactors [7].

In mammals and humans, HDACs play vital roles in cell migration, growth, and survival, and are closely correlated with various diseases such as tumors, cancers, a group of diseases related to metabolic abnormalities, and so on [6, 14, 15]. HDAC inhibitors (HDACi) can repress histone deacetylation mediated by HDAC through several different approaches and have been studied widely to apply in diverse diseases therapy. According to the different structures and characteristics of the HDAC subfamilies, a variety of HDACi were identified and designed to cure human

diseases [16-19]. Some HDACs function with zinc in their catalytic site, hence, the main target of HDAC inhibitors is to suppress the inherent activity of HDACs by occupying the catalytic core of the Zn^{2+} binding site [14, 20, 21]. Trichostatin A (TSA) and vorinostat [suberoylanilide hydroxamic acid (SAHA)] have been identified to inhibit HDACs catalytic activity, among which, TSA was the first discovered natural hydroxamate and HDACi used in treating patients with malignancy successfully together with vorinostat (e.g., cutaneous T-cell lymphoma) [6, 22, 23]. Furthermore, some aminosuberoyl hydroxamic acids have shown the ability to repress HDACs and cell proliferation at nanomolar concentrations [20], facilitating the application of HDACi in disease therapy. Basically, HDACi promotes the accumulation of acetylated histones and non-histone proteins that are involved in the regulation of gene expression, enzymatic activity, cell proliferation, and so on. Even so, the molecular mechanisms underlying the HDACi-mediated cell growth retardation and cell death associated with antitumor are complex and not completely elucidated [16, 24-26]. The development of small molecule HDACi for various disease conditions including cancer is an emerging target in recent times [15].

In insects, life-history traits such as longevity and fecundity are severely affected by the suppression of HAT/HDAC activity, achieved by the application of chemical inhibitors. Bea aphid (*Acyrthosiphon pisum*)-a model insect often is used to study complex life-history traits. Specific chemical inhibitors of HATs/HDACs showed a remarkably severe impact on life-history traits including reducing survival, delaying development, and limiting the number of offspring. The selective inhibition of HATs

and HDACs also had opposing effects on aphid body weight [4].

Furthermore, many studies have proved that HDACs play critical and versatile roles in plant development including seed germination, vegetative and reproduction tissues development, trichome, and root hair cell differentiation as well as abiotic stress tolerance [1, 2, 4, 5, 27]. In *Arabidopsis*, it also showed that TSA and diallyl disulfide (DADS) inhibited the seedling development in MS medium [27]. In rice, using TSA resulted in impaired callus formation of mature embryos and increased global histone H3 acetylation levels, decreased auxin response, and cell proliferation in callus formation [28]. Cotton fiber, the principal natural resource for the textile industry, is also an excellent model to study cell differentiation and development. Thirty HDAC genes were identified from the tetraploid variety *Gossypium hirsutum*, and GhHDA5 has been shown the negative regulation on fiber cell differentiation, indicating some clues for the mechanisms of HDACs and the crucial roles of histone deacetylation in fiber development [5]. However, the underlying mechanism associated with histone deacetylation for fiber development is unclear.

The application of HDACi in plants also provided some interesting results. For example, Plant cell cultures are good for the output of recombinant proteins, with lower costs than mammalian cells except the only flaw of the low yields obtained. After adding HDACi in the culture, higher levels of transgene expression and protein accumulation were observed, showing HDACi as an enhancer of recombinant protein production in plant cell suspensions, which offers the potential to improve the yields of the recombinant protein in plant cell cultures with epigenetic strategies [29],

evidencing the correlation between histone acetylation and increased transcription levels and production of recombinant proteins. Moreover, TSA showed negative roles in fiber development through *in vitro* culture of ovules [5], supporting the key role of histone deacetylation in fiber development.

Here, the HDACi-TSA was used for in *vitro* culture of ovules after and before fiber cells initiation (i.e. ovules at 0 DPA and -2 DPA) and the results revealed that TSA inhibits not only fiber elongation but also fiber cell initiation and differentiation. The succedent transcriptomic analysis identified some phytohormone and secondary metabolism-related genes, which may play important roles in fiber development through histone deacetylation-mediated pathways and some complicated interactions.

Results:

In vitro TSA treatment of ovule inhibits fiber initiation and earlier elongation

The previous study has shown the important roles of TSA in fiber elongation [5], but the effect of TSA in fiber cell initiation and the underlying mechanisms are yet unclear. We used the ovules before and after anthesis (-2 DPA and 0 DPA, respectively) to test the roles of TSA for fiber cell initiation and earlier elongation. The results showed that TSA significantly inhibits the fiber cell initiation as well as the earlier fiber elongation compared with mock *in vitro* culture (Fig. 1), indicating the important roles of histone deacetylation in fiber cell initiation. The long-term *in vitro* culture of 0 DPA ovules further confirmed the inhibition of TSA on the fiber elongation (Fig. S1). Subsequently, the ovules of -2 DPA treated with TSA (10 μM) for 6 days *in vitro*

133 culture were used for RNA extraction and RNA-Seq with Illumina sequencing
134 platform.

135 **RNA-Seq of ovules after TSA treatment and data analysis**

136 In total, more than 9.01G of clean data for each sample was obtained. The clean reads
137 were used to assemble the transcriptome for each sample by mapping the reads to the
138 cotton reference genome (http://mascotton.njau.edu.cn/info/1054/1118.htm). More
139 than 90.0% of the reads could be mapped to the cotton reference genome, and more
140 than 75%, approximately 20%, and 4% of the mapped reads were mapped to exon,
141 intergenic, and intron regions, respectively (Fig. 2A). The mapped reads from all
142 samples were then remapped to the reference genome and 77, 691 unigenes were
143 defined by assembling clean reads with Trinity. All unigenes obtained by
144 transcriptome sequencing were annotated into the NR, KEGG, GO, COG, eggNOG,
145 Swiss-Prot, Pfam, and KOG databases. As a result, 77,555 (NR: 99.82%), 28,174
146 (KEGG: 36.26%), 57,846 (GO: 74.46%), 26,087 (COG: 33.58%), 70,960 (eggNOG:
147 91.34%), 55,767 (Swiss-Prot: 71.77%), 59,214 (Pfam: 76.22%) and 41,302 (KOG:
148 53.16%) unigenes were functionally annotated, respectively. In the NR database, the
149 results showed that *G. hirsutum* had the highest matching degree with the unigene
150 sequence (47.92%), followed by *G. ramondii* (23%), *G. barbadense* (15.12%), and *G.*
151 *arboretum* (11.66%). The matched genes are less than 2% in other close species (i.e.
152 *Durio zibethinus*, *Theobroma cacao*, *Corchorus olitorius*, *Herrania umbratica*), and
153 1.78% of the unigenes did not match the protein sequences of other species (Fig. 2B),
154 indicating the accuracy of RNA-Seq and some specificity of the cotton genes.

Alternative splicing (AS), generating distinct mRNA species and non-coding RNAs (ncRNAs) from one primary transcript, functions as an additional regulatory mechanism for gene expression and function after transcription, which endow AS with importance for bringing protein and function diversity from a definite gene [39]. The conserved AS events were identified and 12 types of AS events were found in all the samples. Two types of ASs at 5' first exon (TSS, transcription start site) and 3' last exon (TTS, transcription terminal site) are the most; then followed by alternative exon ends (AE) at 5' end, 3' end, or both and intron retention (IR) (Fig. 3), which indicated the various and complicated regulatory mechanisms of gene post-transcription.

Analysis of differentially expressed genes in ovules after TSA treatment

To explore the underlying mechanisms of TSA inhibiting fiber initiation, DEG were identified between mock and TSA-treated ovules. The MA plots showed that most genes did not change in transcription level (black plots); the numbers of up-regulated and down-regulated genes were similar with significant alteration of transcription (red and green plots) (Fig. S2). Totally, 4,209 genes were identified with 2,025 genes up-regulated and 2,184 down-regulated, respectively, in response to TSA. Among which 4,196 genes were annotated including 3,980 known genes and 216 new genes (annotated), as well as 13 unknown genes (without annotation and locus) (Table 1 and Table S2). To illuminate the potent causal pathways and key genes, KEGG enrichment pathway analysis was performed. The up-regulated genes were classified into 95 pathways among five categories: cell process, environmental information processing, genetic information processing, metabolism, and organismal systems, and

177 the top 50 pathways in five categories were presented (Fig. 4A). Metabolism
178 accounted for the largest proportion among the categories. Furthermore, the plant
179 hormone signal transduction (46 genes) and phenylpropanoid biosynthesis pathways
180 (51 genes) showed the most genes. The statistics analysis of pathway enrichment
181 showed the lowest q-value (red color) and higher rich factor of plant hormone signal
182 transduction and phenylpropanoid biosynthesis pathways also indicated the reliable
183 enrichment significance (Fig. 4A). For the down-regulated genes, which were
184 classified into 97 pathways among five categories as same as above, and the top 50
185 pathways in five categories were represented. The plant hormone signal transduction
186 (48 genes), photosynthesis (41 genes), and Carbon metabolism pathways (39 genes)
187 showed the most genes. The statistics analysis of the three enrichment pathways
188 showed their lowest q-value and the reliable significance of enrichment pathways (Fig.
189 4B). From the above results, a lot of genes related to plant hormone signal
190 transduction may play important roles in the initial ovule and fiber development
191 mediated by histone deacetylation. Moreover, up-regulated DEGs were also largely
192 enriched in phenylpropanoid biosynthesis (Fig. 4A); while, carbon metabolism, and
193 photosynthesis-related genes were enriched in the down-regulated genes (Fig. 4B),
194 providing evidence that histone deacetylation functions upstream of diverse
195 metabolism pathways to regulate fiber initiation.

196 **Several phytohormonal pathways play important roles in fiber initiation**
197 **downstream of histone deacetylation**

198 In total, up-and down-regulated 94 DEG associated with hormone signal transduction

were used to draw the heatmap with the FPKM values in all the samples (Fig. 5 and Table S3). The resulting heatmap divided the DEGs into four classifications a, b, c, and d. In class a, the genes were significantly up-regulated in response to TSA treatment; while genes were significantly down-regulated in response to TSA treatment in class d. In clades b and c, the difference of transcription level is less weak in ovules of Mock compared with TSA treatments, while the difference is also significant. The FPKM values of each gene in b class were less than 6, while those were more than 8 in class c (Table S4).

To understand the detailed hormonal pathways, we analyzed the down-and up-regulated genes. It is shown that most of the down-regulated genes are related with auxin pathway including small auxin up-regulated RNA (SAUR), INDOLE-3-ACETIC ACID INDUCIBLE (IAA), AUXIN RESPONSE FACTOR (ARF), auxin receptor, and genes associated with IAA synthesis and homeostasis accounting for about 65.4 % of the down-regulated genes, indicating the positive role of auxin in fiber initiation (Table 2). Interestingly, among the up-regulated members, auxin-related genes (e.g., small auxin up-regulated RNA and auxin influx carrier), The JASMONATE-ZIM DOMAIN (JAZ)-Like factors associated with JASMONIC ACID (JA), ABA associated genes (e.g., ABA receptors, signaling factors) account for 32.6%, 30.4%, and 15.2%, respectively; furthermore, three GA receptor were also showed a clearly up-regulated expression (Table 3). Collectively, auxin plays important positive roles in fiber initiation downstream of histone deacetylation; whereas, some small auxin up-regulated RNA encoding genes and auxin influx

carriers also play negative roles in fiber initiation. ABA pathways and JA inhibitory factor JAZ2 play negative roles in fiber initiation downstream of histone deacetylation similar to the previous studies [38, 40, 41], which suggested that histone deacetylation plays a vital role in fiber initiation and earlier elongation through regulating various phytohormones signaling pathways.

Moreover, some key genes transcription expression in phytohormone pathways was validated in TSA-treated ovules with quantitative PCR (Fig. 6). The results showed that some genes such as *GhIAA3_A1*0, *GhIAA19_D10*, *GhSAUR1_D02,* and *GhSAUR12_D12* were down-regulated significantly, while some genes including *GhAUX1_A01*, *GhSAUR50_A03*, *GhSAUR31_A12*, and *GhSAUR8_D02* were up-regulated clearly in the auxin signaling pathway. Two ethylene response factors *GhERF1B* and *GhERF1_D02* as well as four negative regulators in the JA pathway-JAZ protein-coding genes *GhJAZ1_A08/D05* and *GhJAZ10_A03/D02* showed obvious up-regulation. Two factors in gibberellins (GA) pathways *GhGID1_A08* and *GhPIF3_A07* showed up-and down-regulation respectively in TSA-treated ovules. Four abscisic acids (ABA) signaling genes *GhSRK2E_D11*, *GhPYL5_D10*, *GhPYL6_A06,* and *GhAHG1_A12* showed significant up-regulation in response to TSA treatment. All the results point out the crucial roles of different phytohormones downstream of histone deacetylation in fiber initiation.

Regulation of different plant hormones on fiber initiation and development

To further verify the important role of phytohormones in regulating fiber initiation and elongation, the ovules of -2 DPA were incubated in BT- medium with different

243 treatments *in vitro*, including GA3 or IAA deficient, and supplemented with 20 μM
244 ABA or Methyl Jasmonate (MeJA) of different concentration gradients (0.05, 0.5 μM)
245 for 7 or 14 days. After analysis, fiber initiation and development were both severely
246 inhibited in BT medium without GA3 and IAA, especially for GA3. Similarly, no
247 fiber initiated after 7 days of culture, but little fiber was present after 14 days in
248 response to 20 μM ABA (Fig. 7A). However, in the medium containing MeJA (0.05,
249 0.5 μM), the fiber lengths were more than that in the medium mock. Among them,
250 0.05 uM MeJA promoted fiber elongation most effectively (Fig. 7B). These results
251 demonstrated the positive regulation of GA, auxin and MeJA and the inhibitory effect
252 of ABA on fiber initiation and development.

253 **Discussion**

254 Cotton fiber is one of the most important cash products worldly and the model for cell
255 differentiation and elongation study [42]. Lots of researches have been carried out to
256 clarify the underlying mechanism of fiber development, and many important genes
257 have been identified involved in the different pathways to regulate fiber cell initiation,
258 elongation, secondary cell wall deposition, and maturation [5, 38, 43]. Among the
259 pathways involved in fiber development, histone (de)acetylation, one of the important
260 epigenetic modifications is also playing the crucial roles, and HDA5 was identified as
261 a key histone deacetylase in fiber initiation [5, 44]. In total, eighteen HATs and thirty
262 HDACs were identified from *G. hirsutum* [5, 45], however, the detailed roles of
263 different HAT or HDAC and the associated regulatory network are yet unclear.

264 **HDACi-TSA represses the fiber initiation and earlier elongation significantly**

Due to the important roles of histone acetylation in eukaryotes development, HDACi, which can repress histone deacetylation , have been applied in eukaryote development studies and diseases therapy [4, 20, 26-28]. *In vitro* culture of ovules, the application of TSA also showed its repressive role in fiber elongation [5]. Here, we used TSA *in vitro* culture of ovules before and after anthesis, and the results showed that TSA inhibits the fiber cell initiation as well as the primary elongation (Fig.1). These findings indicate that histone acetylation bona fide plays significant role in fiber development and forward us to explore the underlying mechanisms, then, an RNA-Seq was made using the ovules treated with TSA and Mock.

DEGs analysis in the ovule after TSA treatment through RNA-Seq

From the libraries, a total of 77,691 genes were identified, which is very close to the gene numbers in the whole genome and indicates the higher library quality. Analysis of the mapped reads showed that about 23% of reads were mapped intergenic and intron regions, which implied that some possible new genes were identified from the libraries of ovules. The alternative splicing analysis of transcripts displayed that TSS and TTS types are the most AS types in cotton, which is not the same with previous studies [46-48]. In *Arabidopsis* and rice, 'Intron retention' was the prevalent type [47, 49, 50]. By contrast, 'exon skipping' is the most dominant pattern in humans and yeast [46, 48], which proposed that AS varies during the eukaryote evolution.

The DEGs in response to TSA treatment were identified to illuminate the underlying mechanism of fiber initiation involved by histone deacetylation. Totally, 4,209 DEGs including 229 new genes consisting of 216 annotated genes and 13 genes

without annotation and locus information were found, which implied that the public genome data is still not perfect and the more advanced technology of assembly is necessary. Then, a KEGG analysis was operated and the results showed that plant hormone signal transduction, phenylpropanoid biosynthesis, and glutathione metabolism are the most enriched groups in up-regulated genes; in contrast, plant hormone signal transduction, carbon metabolism, and photosynthesis are the most enriched groups in the down-regulated genes (Fig. 4). Phenylpropanoid pathway is associated with flavonoid biosynthesis, which competes with the the fatty acid pathway for malonyl-CoA [51, 52], and the fatty acid metabolism mediates the fiber development [53, 54]. Moreover, a previous study demonstrated that flavonoid naringenin is negatively associated with fiber development and that the flavonoid metabolism mediated by flavanone 3-hydroxylase is important in fiber development [55], which is in agreement with our findings and provides clues for the underlying mechanism associated with histone deacetylation. Glutathione (GSH), an α-amino acid and a tripeptide, functions as a molecule that protects cells against oxidation through providing the cell with its reducing milieu, which maintains various cellular components including enzymes in a reduced state, furthermore, glutathione also functions as a storage and transport form of cysteine moieties [56, 57]. Cysteine is a kind of important intermediate of sulfur metabolism in plants and functions as the reduction state of sulfite by the enzyme APS reductase and the cysteine synthase complex, which uses the interaction of the enzymes serine acetyltransferase and O‐acetylserine‐(thiol)‐lyase to control flux through the pathway [58-60]. Therefore,

the up-regulated phenylpropanoid biosynthesis and glutathione metabolism indicate that fatty acid pathway and sulfur metabolism areinvolved in the fiber initiation regulation dependent on histone acetylation at least partially, which supported the previous studies as well as provided novel clues for fiber cell development study [53, 54].

Carbon metabolism and photosynthesis are closely related, which control the energy production, transport, and application in the life cycle of plants [61-63]. The repressive carbon metabolism and photosynthesis after TSA treatment suggest the attenuated energy metabolism in the ovules, which is consistent with the retarded fiber development. More interestingly, the phytohormone signal transduction was enriched in both up-and down-regulated pathways, indicating that different hormones may be involved in the fiber development downstream of histone deacetylation, which is also in line with the previous studies [43, 64, 65].

Histone deacetylation functions upstream of the phytohormones network to regulate fiber development.

Many studies have shown that phytohormones such as auxin, GA, ethylene, cytokinin (CK), brassinosteroids (BR), and ABA play important roles in fiber development [42, 43, 64, 66]. Our RNA-Seq results supported the roles of phytohormones and provided some potential regulatory mechanisms associated with histone acetylation modification. The intensive analysis of the hormone pathway revealed that 49 auxin pathway-related genes showed differential expression including 34 up-regulated and 15 down-regulated after TSA treatment, indicating the dominant role of auxin in fiber

development of cotton, supporting the pivotal role of auxin in fiber cell initiation [67]. In *Arabidopsis*, HDA6, HDA9, and HDA19 have been shown the regulatory roles in transcription expression of *AUX1* and some *ARF*s through histone deacetylation modification to regulate the auxin pathway and seed germination and valve cell elongation [68, 69]. Some *IAA*s are also regulated by histone deacetylation to involve the response to aberrant ambient light and temperature of the plant [70, 71]. Here, *GhAUX1_A01* and some *GhSAUR*s (e.g., *GhSAUR50_A03*, *GhSAUR31_A12*, and *GhSAUR8_D02*) showed up-regulation, indicating the potential auxin import and accumulation of non-fiber cell; while the down-regulation of *GhIAA*s and *GhSAUR*s implied the conceivable repression of auxin signal in fiber cells which inhibits the fiber initiation downstream of histone deacetylation. Interestingly, auxin has been shown the key role in the fiber cell initiation through the proper spatiotemporal accumulation and distribution, in which the auxin efflux carrier PIN3 plays an important positive role; moreover, CK inhibits non-fiber-localized protein GhPIN3a and damages the normal auxin concentration gradient to involve the fiber cells initiation negatively [65, 67]. All the above suggested that different auxin pathway genes play distinct roles in fiber development, and auxin promotes fiber cell initiation through histone acetylation regulation partially.

As an important hormone in plant development and abiotic stress tolerance, ABA also exhibits a negative role in fiber cell development [38, 41, 42, 64], although the underlying mechanism is ambiguous. Here, all the identified ABA pathway genes encoding receptors and signaling factors except *HAB1* (a negative regulator in ABA

353 signaling) were up-regulated encouraging its negative function in fiber initiation, as
354 well as offering the potential epigenetic mechanism upstream of the ABA pathway.
355 JAZ2 is a key negative regulator in cotton fiber initiation [38], some homologues of
356 JAZ2 (e.g., *GhJAZ1_A08/D05* and *GhJAZ10_A03/D02*) showed higher expression
357 after TSA treatment, supporting the negative role of JAZ in fiber initiation and
358 providing the clues between histone deacetylation and JA pathway in fiber initiation.
359 Besides, some genes associated with GA and SA also showed differential expression,
360 raising some clues for the relationship between phytohormones and epigenetic
361 modifications in fiber development. To sum up, a primary schematic diagram was
362 presented to explain the potential regulatory mechanisms between the histone
363 acetylation and phytohormones and other metabolisms for fiber cell initiation and
364 earlier development (Fig. 7). Histone acetylation can modify some genes in different
365 phytohormones to regulate auxin and GA positively, and ABA and JA negatively to
366 mediate fiber cell initiation. Moreover, phenylpropanoid biosynthesis and
367 energy-related metabolisms also function downstream of histone deacetylation to
368 involve fiber initiation development. However, the relationship between
369 phytohormones and different secondary metabolism/carbon metabolisms still needs
370 much work to uncover.

371 **Conclusions**

372 In a word, we highlighted that histone deacetylation inhibitor-trichostatin A (TSA)
373 represses the fiber cell initiation and elongation of cotton in *in vitro* culture, indicating
374 the crucial roles of histone deacetylation in cell differentiation and development.

RNA-Seq revealed that 2,025 genes associated with plant hormone signal transduction and phenylpropanoid biosynthesis, and 2,184 genes associated with plant hormone signal transduction, photosynthesis, and carbon metabolism were up-and down-regulated, respectively, in response to TSA treatment. Further studies showed that TSA repressed the auxin, GA, JA and SA signalings, while promoted ABA signalings to regulate fiber cell initiation and earlier elongation. Phytohormones palys versative roles in plant development including fiber development. Our work demonstrated that histone deacetylation contributed much to the functions and the interactions between different phytohormones in fiber initiation, which is very helpful for us to understand the detailed molecular mechanisms of phytohormone pathways regulation and fiber development.

Materials and Methods

In vitro culture and scanning electron microscopy (SEM) analysis of cotton ovules

Cotton cultivar ZM24 (also as CCRI24), obtained from the Institute of Cotton Research, the Chinese Academy of Agricultural Sciences were grown under field conditions in Zhengzhou China for the following study [30]. Flowers were harvested at -2 and 0 days post-anthesis (DPA), and ovaries were surface sterilized by using 75% ethanol. Ovules were carefully dissected from the ovaries under sterile conditions and immediately floated on liquid BT media supplemented with optimized phytohormone concentrations (5 μM IAA and 0.5 μM GA_3) and various concentrations of TSA in culture plates [31]. The ovules were incubated at 32°C in

397 the dark without agitation. TSA (Millipore, 647925) was dissolved in 95% DMSO to
398 make a 1 mM stock solution. Fiber development for all cultural ovules was analyzed
399 after indication time of incubation by SEM (Hitachi SU3500). Moreover, the cultured
400 ovules with different times were frozen in liquid nitrogen or -80°C condition for the
401 following experiments.

402 **Library preparation, RNA-Seq, and data analysis**

403 Total RNA was extracted from the -2 DPA ovules after 6 days of *in vitro* culture with
404 TSA and the mock. RNA quantification, qualification, and RNA concentration was
405 measured using NanoDrop 2000 (Thermo). RNA integrity was assessed with the RNA
406 Nano 6000 Assay Kit of the Agilent Bioanalyzer 2100 system (Agilent Technologies,
407 CA, USA).

408 A total amount of 1 μg RNA per sample was used as input material for the library
409 construction. Sequencing libraries were generated using NEBNext UltraTM RNA
410 Library Prep Kit for Illumina (NEB, USA) following manufacturer's
411 recommendations by Beijing Biomarker Technologies Co., Ltd (Beijing, China).
412 Total six libraries including three biological repeats each sample were used for the
413 RNA-Seq. Clean data in Illumina sequencing was obtained by removing containing
414 adapter, containing ploy-N and low quality reads from raw data. Only reads with a
415 perfect match or one mismatch were further analyzed and annotated based on the
416 reference genome. Hisat2 tools soft were used to map with reference TM-1 (AD1)
417 genome NAU-NBI (Nanjing Agricultural University-Novogene Bioinformatics
418 Technology) assembly v1.1 and annotated v1.1 (https://www.cottongen.org) [32]. The

raw data can be accessible from the following BioProject ID: PRJNA733691 in the NCBI SAR database.

Alternative splicing was analyzed with the non-redundant transcript sequences, which were directly used to run all-vs-all BLAST with high identity settings. BLAST alignments that met all criteria were considered products of the candidate AS events: (1) both sequence lengths exceeded 1,000 bp and the alignment contained 2 high-scoring segment pairs (HSPs); (2) the alternative splicing gap exceeded 100 bp and was located ≥100 bp from the 3′ /5′ end; and (3) a 5-bp overlap was allowed for all alternative transcripts.

Gene function was annotated against the databases NR (NCBI non-redundant protein sequences), Nt (NCBI non-redundant nucleotide sequences), Pfam (Protein family) [33], KOG/COG (Clusters of Orthologous Groups of proteins), Swiss-Prot (A manually annotated and reviewed protein sequence database), KO (KEGG Ortholog database) and GO (Gene Ontology) [34].

GATK2 or Samtools software was used to perform SNP calling. Raw vcffiles were filtered with GATK standard filter method and other parameters (clusterWindowSize: 10; MQ0 >= 4 and (MQ0/(1.0*DP)) > 0.1; QUAL < 10; QUAL < 30.0 or QD < 5.0 or HRun > 5), and only SNPs with distance > 5 were retained. Quantification of gene expression levelsGene expression levels was estimated by fragments per kilobase of transcript per million fragments mapped. The formula is shown as follow:

$$\mathrm{FPKM} = \frac{\text{cDNA Fragments}}{\text{Mapped Fragments(Millions)} \times \text{Transcript Length(kb)}}$$

Differential expression analysis and KEGG pathway enrichment analysis

Differential expression analysis of two samples (Mock and TSA treatments) was performed using the DEseq [35]. Genes with at least twofold change and an adjusted P-value < 0.01 established by DEseq were assigned as differentially expressed. KEGG (Kyoto Encyclopedia of Genes and Genomes) database and KOBAS software were used to test the statistical enrichment of differential expression genes [36, 37].

RNA extraction and qRT–PCR

Total RNA from cotton ovules was extracted using the Qiagen RNeasy kit and RNAqueous small-scale phenol-free total RNA isolation kit (Ambion) according to the manufacturer's instructions and reverse transcribed using the SuperScript RT-PCR system (Invitrogen). The qRT-PCR for each gene was performed in three biological replicates using the KAPA SYBR FAST qPCR Kits (KAPA) and the expression value was quantified and normalized to the value of UBIQUITIN 7 [38]. Mean values and standard errors for each gene were calculated from three biological replicates. Primers are listed in Supplementary Table 1.

List of abbreviations

ABA : Abscisic Acid ; AE : Alternative exon ends; ARF :Auxin response factor; AS :Alternative splicing;BR: Brassinosteroids; CK:cytokinin; DEGs :Differentially expressed genes; DPA: Days post-anthesis ; GA :Gibberellic Acid ; GO: Gene Ontology; GSH :Glutathione ;HATs :histone acetyltransferases ;HDACs:histone deacetylases; HDACi :HDAC inhibitors; IAA:Indole-3-acetic acd inducible; IR :Intron retention; JA :Jasmonic Acid; JAZ:Jasmonate-zim domain; KEGG : Kyoto

Encyclopedia of Genes and Genomes; KO: KEGG Ortholog database; KOG/COG :Clusters of Orthologous Groups of proteins; MeJA :Methyl Jasmonate; NcRNAs :non-coding RNAs ; NR :NCBI non-redundant protein sequences; Nt: NCBI non-redundant nucleotide sequences; Pfam :Protein family; SA: Salicylic acid; SAHA:suberoylanilide hydroxamic acid; SEM: Scanning electron microscopy; Swiss-Prot :A manually annotated and reviewed protein sequence database; TSA: Trichostatin A; TSS:Transcription start site.

Declaration

Ethics approval and consent to participate

Not applicable.

Consent for publication

Not applicable.

Availability of data and materials

Not applicable.

Competing interests

I declare on behalf of my co-authors that there is no conflict of interest exists in the submission of this manuscript which is approved by all authors.

Funding

This work is supported by the National Natural Science Foundation of China (32072022 and 31690093), the Creative Research Groups of China (31621005), Central Public-interest Scientific Institution Basal Research Fund (1610162020010202), and Zhengzhou University (32410196).

Authors' contributions

Zhi Wang: Conceptualization, Funding acquisition, Methodology, Data curation, Writing - original draft. Zhenzhen Wei and Yonghui Li: Methodology, Data curation, Writing - review & editing. Faiza Ali and Ye Wang: Writing - review & editing. Zuoren Yang: Investigation. Jisheng Liu and Fuguang Li: Resources. All authors have approved the published version of the manuscript.

Acknowledgments

We would like to thank the participants in this study.

References

1. Geng YK, Zhang PX, Liu Q, Wei ZW, Riaz A, Chachar S, et al. Rice homolog of Sin3-associated polypeptide 30, OsSFL1, mediates histone deacetylation to regulate flowering time during short days. Plant Biotechnol J. 2020; 18(2):325-327. http://dx.doi.org/10.1111/pbi.13235

2. Hu Y, Lu Y, Zhao Y.Zhou DX. Histone Acetylation Dynamics Integrates Metabolic Activity to Regulate Plant Response to Stress. Frontiers in plant science. 2019; 10:1236. http://dx.doi.org/10.3389/fpls.2019.01236

3. Huang F, Yuan WY, Tian S, Zheng QJ, He YH. SIN3 LIKE genes mediate long-day induction of flowering but inhibit the floral transition in short days through histone deacetylation in Arabidopsis. Plant J. 2019; 100(1):101-113. http://dx.doi.org/10.1111/tpj.14430

4. Kirfel P, Skaljac M, Grotmann J, Kessel T, Seip M, Michaelis K, et al. Inhibition of histone acetylation and deacetylation enzymes affects longevity, development, and fecundity in the pea aphid (Acyrthosiphon pisum). Arch Insect Biochem. 2020; 103(3). https://doi.org/10.1002/arch.21614

5. Kumar V, Singh B, Singh SK, Rai KM, Singh SP, Sable A, et al. Role of *GhHDA5* in H3K9 deacetylation and fiber initiation in Gossypium hirsutum. Plant J. 2018; 95(6):1069-1083. http://dx.doi.org/10.1111/tpj.14011

6. Marks P, Rifkind RA, Richon VM, Breslow R, Miller T, Kelly WK. Histone deacetylases and cancer: causes and therapies. Nature reviews Cancer. 2001; 1(3):194-202. http://dx.doi.org/10.1038/35106079

7. Ng HH.Bird A Histone deacetylases: silencers for hire. Trends in biochemical sciences. 2000; 25(3):121-126. http://dx.doi.org/10.1016/s0968-0004(00)01551-6

8. Wang Z, Cao H, Chen F, Liu Y. The roles of histone acetylation in seed performance and plant development. Plant physiology and biochemistry : PPB. 2014; 84:125-133. http://dx.doi.org/10.1016/j.plaphy.2014.09.010

9. Johnson CA, Turner BM. Histone deacetylases: complex transducers of nuclear signals. Seminars in cell & developmental biology. 1999; 10(2):179-188. http://dx.doi.org/10.1006/scdb.1999.0299

10. Kolle D, Brosch G, Lechner T, Pipal A, Helliger W, Taplick J, et al. Different types of maize histone deacetylases are distinguished by a highly complex substrate and site specificity. Biochemistry-Us. 1999; 38(21):6769-6773. http://dx.doi.org/10.1021/Bi982702v

11. Lechner T, Lusser A, Pipal A, Brosch G, Loidl A, Goralik-Schramel M, et al. RPD3-type histone

524 deacetylases in maize embryos. Biochemistry-Us. 2000; 39(7):1683-1692.
525 https://doi.org/10.1021/bi9918184
526 12. Lusser A, Brosch G, Loidl A, Haas H, Loidl P. Identification of maize histone deacetylase HD2 as
527 an acidic nucleolar phosphoprotein. Science. 1997; 277(5322):88-91.
528 http://dx.doi.org/10.1126/science.277.5322.88
529 13. Wu KQ, Tian LN, Malik K, Brown D.Miki B Functional analysis of HD2 histone deacetylase
530 homologues in *Arabidopsis thaliana*. Plant J. 2000; 22(1):19-27.
531 https://doi.org/10.1046/j.1365-313x.2000.00711.x
532 14. An XL, Wei ZK, Ran BT, Tian H, Gu HY, Liu Y, et al. Histone Deacetylase Inhibitor Trichostatin A
533 Suppresses Cell Proliferation and Induces Apoptosis by Regulating the PI3K/AKT Signalling
534 Pathway in Gastric Cancer Cells. Anti-Cancer Agent Me. 2020; 20(17):2114-2124.
535 http://dx.doi.org/10.2174/1871520620666200627204857
536 15. Sarkar R, Banerjee S, Amin SA, Adhikari N, Jha T. Histone deacetylase 3 (HDAC3) inhibitors as
537 anticancer agents: A review. Eur J Med Chem. 2020; 192.
538 https://doi.org/10.1016/j.ejmech.2020.112171
539 16. Bolden JE, Peart MJ, Johnstone RW. Anticancer activities of histone deacetylase inhibitors.
540 Nature reviews Drug discovery. 2006; 5(9):769-784. http://dx.doi.org/10.1038/nrd2133
541 17. Dokmanovic M, Marks PA. Prospects: histone deacetylase inhibitors. Journal of cellular
542 biochemistry. 2005; 96(2):293-304. http://dx.doi.org/10.1002/jcb.20532
543 18. Miller TA, Witter DJ, Belvedere S. Histone deacetylase inhibitors. Journal of medicinal
544 chemistry. 2003; 46(24):5097-5116. http://dx.doi.org/10.1021/jm0303094
545 19. Rasheed WK, Johnstone RW, Prince HM. Histone deacetylase inhibitors in cancer therapy.

546 Expert opinion on investigational drugs. 2007; 16(5):659-678.
547 http://dx.doi.org/10.1517/13543784.16.5.659
548 20. Belvedere S, Witter DJ, Yan J, Secrist JP, Richon V, Miller TA. Aminosuberoyl hydroxamic acids
549 (ASHAs): a potent new class of HDAC inhibitors. Bioorganic & medicinal chemistry letters.
550 2007; 17(14):3969-3971. http://dx.doi.org/10.1016/j.bmcl.2007.04.089
551 21. Yoon S, Eom GH HDAC and HDAC. Inhibitor: From Cancer to Cardiovascular Diseases.
552 Chonnam medical journal. 2016; 52(1):1-11. http://dx.doi.org/10.4068/cmj.2016.52.1.1
553 22. Duvic M, Talpur R, Ni X, Zhang C, Hazarika P, Kelly C, et al. Phase 2 trial of oral vorinostat
554 (suberoylanilide hydroxamic acid, SAHA) for refractory cutaneous T-cell lymphoma (CTCL).
555 Blood. 2007; 109(1):31-39. http://dx.doi.org/10.1182/blood-2006-06-025999
556 23. Richon VM, Emiliani S, Verdin E, Webb Y, Breslow R, Rifkind RA, et al. A class of hybrid polar
557 inducers of transformed cell differentiation inhibits histone deacetylases. Proceedings of the
558 National Academy of Sciences of the United States of America. 1998; 95(6):3003-3007.
559 http://dx.doi.org/10.1073/pnas.95.6.3003
560 24. Dokmanovic M, Clarke C, Marks PA. Histone deacetylase inhibitors: Overview and
561 perspectives. Mol Cancer Res. 2007; 5(10):981-989.
562 http://dx.doi.org/10.1158/1541-7786.MCR-07-0324
563 25. Kaushik D, Vashistha V, Isharwal S, Sediqe SA, Lin MF. Histone deacetylase inhibitors in
564 castration-resistant prostate cancer: molecular mechanism of action and recent clinical trials.
565 Therapeutic advances in urology. 2015; 7(6):388-395.
566 http://dx.doi.org/10.1177/1756287215597637
567 26. Marks PA, Breslow R. Dimethyl sulfoxide to vorinostat: Development of this histone

568 deacetylase inhibitor as an anticancer drug. Nat Biotechnol. 2007; 25(1):84-90.
569 http://dx.doi.org/10.1038/nbt1272
570 27. Wang Z, Cao H, Sun Y, Li X, Chen F, Carles A, et al. Arabidopsis paired amphipathic helix
571 proteins SNL1 and SNL2 redundantly regulate primary seed dormancy via abscisic
572 acid-ethylene antagonism mediated by histone deacetylation. The Plant cell. 2013;
573 25(1):149-166. http://dx.doi.org/10.1105/tpc.112.108191
574 28. Zhang HD, Guo F, Qi PP, Huang YZ, Xie YY, Xu L, et al. *OsHDA710*-Mediated Histone
575 Deacetylation Regulates Callus Formation of Rice Mature Embryo. Plant Cell Physiol. 2020;
576 61(9):1646-1660. http://dx.doi.org/10.1093/pcp/pcaa086
577 29. Santos RB, Pires AS, Abranches R. Addition of a histone deacetylase inhibitor increases
578 recombinant protein expression in plant cell cultures. Free Radical Bio Med. 2018;
579 120:S135-S135. http://dx.doi.org/10.1016/j.freeradbiomed.2018.04.444
580 30. Yang Z, Zhang C, Yang X, Liu K, Wu Z, Zhang X, et al. *PAG1*, a cotton brassinosteroid catabolism
581 gene, modulates fiber elongation. The New phytologist. 2014; 203(2):437-448.
582 http://dx.doi.org/10.1111/nph.12824
583 31. Beasley CA, Ting IP. EFFECTS OF PLANT GROWTH SUBSTANCES ON IN VITRO FIBER
584 DEVELOPMENT FROM UNFERTILIZED COTTON OVULES. American Journal of Botany. 1974;
585 61(2):188-194. http://dx.doi.org/https://doi.org/10.1002/j.1537-2197.1974.tb06045.x
586 32. Yu J, Jung S, Cheng CH, Ficklin SP, Lee T, Zheng P, et al. CottonGen: a genomics, genetics and
587 breeding database for cotton research. Nucleic Acids Res. 2014; 42(Database
588 issue):D1229-1236. http://dx.doi.org/10.1093/nar/gkt1064
589 33. El-Gebali S, Mistry J, Bateman A, Eddy SR, Luciani A, Potter SC, et al. The Pfam protein

families database in 2019. Nucleic Acids Res. 2019; 47(D1):D427-D432. http://dx.doi.org/10.1093/nar/gky995

34. Young MD, Wakefield MJ, Smyth GK, Oshlack A. Gene ontology analysis for RNA-seq: accounting for selection bias. Genome biology. 2010; 11(2):R14. http://dx.doi.org/10.1186/gb-2010-11-2-r14

35. Anders S, Huber W. Differential expression analysis for sequence count data. Genome biology. 2010; 11(10):R106. http://dx.doi.org/10.1186/gb-2010-11-10-r106

36. Mao XZ, Cai T, Olyarchuk JG, Wei LP. Automated genome annotation and pathway identification using the KEGG Orthology (KO) as a controlled vocabulary. Bioinformatics. 2005; 21(19):3787-3793. http://dx.doi.org/10.1093/bioinformatics/bti430

37. Kanehisa M, Araki M, Goto S, Hattori M, Hirakawa M, Itoh M, et al. KEGG for linking genomes to life and the environment. Nucleic Acids Res. 2008; 36(Database issue):D480-484. http://dx.doi.org/10.1093/nar/gkm882

38. Hu H, He X, Tu L, Zhu L, Zhu S, Ge Z, et al. *GhJAZ2* negatively regulates cotton fiber initiation by interacting with the R2R3-MYB transcription factor GhMYB25-like. Plant J. 2016; 88(6):921-935. http://dx.doi.org/10.1111/tpj.13273

39. Zhu LY, Zhu YR, Dai DJ, Wang X, Jin HC. Epigenetic regulation of alternative splicing. American journal of cancer research. 2018; 8(12):2346-2358PMC6325479

40. Li Y, Tu L, Ye Z, Wang M, Gao W, Zhang X. A cotton fiber-preferential promoter, *PGbEXPA2*, is regulated by GA and ABA in Arabidopsis. Plant cell reports. 2015; 34(9):1539-1549. http://dx.doi.org/10.1007/s00299-015-1805-x

41. Wang YH, Liu JJ, Chen BL, Zhou ZG. Physiological mechanisms of growth regulators 6-BA and

ABA in mitigating low temperature stress of cotton fiber development. Ying yong sheng tai xue bao = The journal of applied ecology. 2011; 22(5):1233-1239

42. Kim HJ, Triplett BA. Cotton fiber growth in planta and in vitro. Models for plant cell elongation and cell wall biogenesis. Plant physiology. 2001; 127(4):1361-1366. https://doi.org/10.1104/pp.010724

43. Wang Z, Yang Z, Li F. Updates on molecular mechanisms in the development of branched trichome in *Arabidopsis* and nonbranched in *cotton*. Plant Biotechnol J. 2019; 17(9):1706-1722. http://dx.doi.org/10.1111/pbi.13167

44. Singh PK, Gao W, Liao P, Li Y, Xu FC, Ma XN, et al. Comparative acetylome analysis of wild-type and fuzzless-lintless mutant ovules of upland cotton (*Gossypium hirsutum* Cv. Xu142) unveils differential protein acetylation may regulate fiber development. Plant physiology and biochemistry : PPB. 2020; 150:56-70. http://dx.doi.org/10.1016/j.plaphy.2020.02.031

45. Imran M, Shafiq S, Farooq MA, Naeem MK, Widemann E, Bakhsh A, et al. Comparative Genome-wide Analysis and Expression Profiling of Histone Acetyltransferase (HAT) Gene Family in Response to Hormonal Applications, Metal and Abiotic Stresses in Cotton. Int J Mol Sci. 2019; 20(21). http://dx.doi.org/10.3390/ijms20215311

46. Sultan M, Schulz MH, Richard H, Magen A, Klingenhoff A, Scherf M, et al. A global view of gene activity and alternative splicing by deep sequencing of the human transcriptome. Science. 2008; 321(5891):956-960. http://dx.doi.org/10.1126/science.1160342

47. Wang BB, Brendel V. Genomewide comparative analysis of alternative splicing in plants. Proceedings of the National Academy of Sciences of the United States of America. 2006; 103(18):7175-7180. http://dx.doi.org/10.1073/pnas.0602039103

634 48. Wang ET, Sandberg R, Luo S, Khrebtukova I, Zhang L, Mayr C, et al. Alternative isoform
635 regulation in human tissue transcriptomes. Nature. 2008; 456(7221):470-476.
636 http://dx.doi.org/10.1038/nature07509
637 49. Ner-Gaon H, Halachmi R, Savaldi-Goldstein S, Rubin E, Ophir R, Fluhr R. Intron retention is a
638 major phenomenon in alternative splicing in Arabidopsis. Plant J. 2004; 39(6):877-885.
639 http://dx.doi.org/10.1111/j.1365-313X.2004.02172.x
640 50. Yang W, Yoon J, Choi H, Fan Y, Chen R, An G. Transcriptome analysis of
641 nitrogen-starvation-responsive genes in *rice*. BMC plant biology. 2015; 15:31.
642 http://dx.doi.org/10.1186/s12870-015-0425-5
643 51. Deschamps C, Simon JE. Phenylpropanoid biosynthesis in leaves and glandular trichomes of
644 basil (Ocimum basilicum L.). Methods in molecular biology. 2010; 643:263-273.
645 http://dx.doi.org/10.1007/978-1-60761-723-5_18
646 52. Vogt T. Phenylpropanoid biosynthesis. Molecular plant. 2010; 3(1):2-20.
647 http://dx.doi.org/10.1093/mp/ssp106
648 53. Qin YM, Hu CY, Pang Y, Kastaniotis AJ, Hiltunen JK, Zhu YX. Saturated very-long-chain fatty
649 acids promote cotton fiber and Arabidopsis cell elongation by activating ethylene
650 biosynthesis. The Plant cell. 2007; 19(11):3692-3704.
651 http://dx.doi.org/10.1105/tpc.107.054437
652 54. Wang XC, Li Q, Jin X, Xiao GH, Liu GJ, Liu NJ, et al. Quantitative proteomics and
653 transcriptomics reveal key metabolic processes associated with cotton fiber initiation. Journal
654 of proteomics. 2015; 114:16-27. http://dx.doi.org/10.1016/j.jprot.2014.10.022
655 55. Tan JF, Tu LL, Deng FL, Hu HY, Nie YC, Zhang XL. A Genetic and Metabolic Analysis Revealed

656 that Cotton Fiber Cell Development Was Retarded by Flavonoid Naringenin. Plant physiology.
657 2013; 162(1):86-95. http://dx.doi.org/10.1104/pp.112.212142
658 56. Meister A. Glutathione metabolism. Methods in enzymology. 1995; 251:3-7.
659 http://dx.doi.org/10.1016/0076-6879(95)51106-7
660 57. Schoenberg MH, Buchler M, Pietrzyk C, Uhl W, Birk D, Eisele S, et al. Lipid peroxidation and
661 glutathione metabolism in chronic pancreatitis. Pancreas. 1995; 10(1):36-43.
662 http://dx.doi.org/10.1097/00006676-199501000-00005
663 58. Crawhall JC, Purkiss P, Stanbury JB. Metabolism of sulfur-containing amino acids in a patient
664 excreting -mercaptolactate-cysteine disulfide. Biochemical medicine. 1973; 7(1):103-111.
665 http://dx.doi.org/10.1016/0006-2944(73)90105-1
666 59. Stipanuk MH. Sulfur amino acid metabolism: pathways for production and removal of
667 homocysteine and cysteine. Annual review of nutrition. 2004; 24:539-577.
668 http://dx.doi.org/10.1146/annurev.nutr.24.012003.132418
669 60. Thomas SA, Catty P, Hazemann JL, Michaud-Soret I, Gaillard JF. The role of cysteine and
670 sulfide in the interplay between microbial Hg(ii) uptake and sulfur metabolism. Metallomics :
671 integrated biometal science. 2019; 11(7):1219-1229. http://dx.doi.org/10.1039/c9mt00077a
672 61. Friedl MA, Schmoll M, Kubicek CP, Druzhinina IS. Photostimulation of Hypocrea atroviridis
673 growth occurs due to a cross-talk of carbon metabolism, blue light receptors and response to
674 oxidative stress. Microbiology. 2008; 154(Pt 4):1229-1241.
675 http://dx.doi.org/10.1099/mic.0.2007/014175-0
676 62. Singh AK, Elvitigala T, Bhattacharyya-Pakrasi M, Aurora R, Ghosh B, Pakrasi HB. Integration of
677 carbon and nitrogen metabolism with energy production is crucial to light acclimation in the

678 cyanobacterium Synechocystis. Plant physiology. 2008; 148(1):467-478.
679 http://dx.doi.org/10.1104/pp.108.123489
680 63. Vargas WA, Pontis HG, Salerno GL. New insights on sucrose metabolism: evidence for an
681 active A/N-Inv in chloroplasts uncovers a novel component of the intracellular carbon
682 trafficking. Planta. 2008; 227(4):795-807. http://dx.doi.org/10.1007/s00425-007-0657-1
683 64. Kim HJ, Hinchliffe DJ, Triplett BA, Chen ZJ, Stelly DM, Yeater KM, et al. Phytohormonal
684 networks promote differentiation of fiber initials on pre-anthesis cotton ovules grown in vitro
685 and in planta. PloS one. 2015; 10(4):e0125046.
686 http://dx.doi.org/10.1371/journal.pone.0125046
687 65. Zeng J, Zhang M, Hou L, Bai W, Yan X, Hou N, et al. Cytokinin inhibits cotton fiber initiation via
688 disrupting PIN3a-mediated IAA asymmetric accumulation in ovule epidermis. Journal
689 of Experimental Botany 2019; 70:13. https://doi.org/10.1093/jxb/erz162
690 66. Sun Y, Veerabomma S, Abdel-Mageed HA, Fokar M, Asami T, Yoshida S, et al. Brassinosteroid
691 regulates fiber development on cultured cotton ovules. Plant Cell Physiol. 2005;
692 46(8):1384-1391. http://dx.doi.org/10.1093/pcp/pci150
693 67. Zhang M, Zheng X, Song S, Zeng Q, Hou L, Li D, et al. Spatiotemporal manipulation of auxin
694 biosynthesis in cotton ovule epidermal cells enhances fiber yield and quality. Nat Biotechnol.
695 2011; 29(5):453-458. http://dx.doi.org/10.1038/nbt.1843
696 68. Wang Z, Chen FY, Li XY, Cao H, Ding M, Zhang C, et al. *Arabidopsis* seed germination speed is
697 controlled by SNL histone deacetylase-binding factor-mediated regulation of AUX1. Nature
698 communications. 2016; 7. https://doi.org/10.1038/ncomms13412
699 69. Yuan LB, Chen X, Chen HH, Wu KQ, Huang SZ. Histone deacetylases HDA6 and HDA9

coordinately regulate valve cell elongation through affecting auxin signaling in *Arabidopsis*. Biochem Bioph Res Co. 2019; 508(3):695-700. http://dx.doi.org/10.1016/j.bbrc.2018.11.082

70. Benhamed M, Bertrand C, Servet C, Zhou DX. Arabidopsis *GCN5*, *HD1*, and *TAF1/HAF2* interact to regulate histone acetylation required for light-responsive gene expression. The Plant cell. 2006; 18(11):2893-2903. http://dx.doi.org/10.1105/tpc.106.043489

71. Shen Y, Lei T, Cui X, Liu X, Zhou S, Zheng Y, et al. Arabidopsis histone deacetylase *HDA15* directly represses plant response to elevated ambient temperature. Plant J. 2019; 100(5):991-1006. http://dx.doi.org/10.1111/tpj.14492

Figure legend:

Fig. 1 Application of TSA repress fiber cell initiation and elongation *in vitro*

(A) -2 DPA (days post anthesis) ovules were treated with 10 u M TSA for 6 days *in vitro*, then the ovule surface was observed and captured by Scanning Electron Microscope. (B) 0 DPA ovules were treated with 10 μM TSA for 2 days *in vitro*, and the ovule surface was observed and captured by SEM. Bar=1 mm (intact ovules) and Bar=200 μm (magnification). The pictures on the right were the magnification of the regions in the left pictures.

Fig. 2 Reads distribution in the genome and natural species distribution of identified genes

(A) All the reads obtained were mapped to the cotton genome, and reads distribution in exon, intergenic, and intron regions were represented for ovules treatment with mock and TSA.

721 (B) A total of 77,555 unigenes were annotated to the Nr protein database. For the
722 species distribution, about 31,720 (47.92%), 17,814(23%), 11,715 (15.12%), and
723 9030 (11.66%) unigenes were mathched with *Gossypium hirsutum*, *G. ramondii, G.*
724 *barbadense* and *G. arboretum*. The matched genes are less than 2% in other close
725 species (i.e. *Durio zibethinus*, *Theobroma cacao*, *Corchorus olitorius*, *Herrania*
726 *umbratica*).

727 **Fig. 3 Alternative splicing analysis of transcripts identified in Mock and TSA**
728 **treated ovules**

729 In the six libraries including mock and TSA treated, alternative splicing of the
730 transcripts was analyzed. In total, 12 kinds of AS events were defined as follows, and
731 the results showed that TSS and TSS are the dominant AS events identified.

732 (1) TSS: Alternative 5'first exon (transcription start site) ;

733 (2) TTS: Alternative 3' last exon (transcription terminal site);

734 (3) SKIP: Skipped exon(SKIP_ON, SKIP_OFF pair);

735 (4) XSKIP: Approximate SKIP (XSKIP_ON, XSKIP_OFF pair) ;

736 (5) MSKIP: Multi-exon SKIP (MSKIP_ON, MSKIP_OFF pair);

737 (6) XMSKIP: Approximate MSKIP (XMSKIP_ON, XMSKIP_OFF pair);

738 (7) IR: Intron retention (IR_ON, IR_OFF pair);

739 (8) XIR: Approximate IR (XIR_ON, XIR_OFF pair);

740 (9) MIR: Multi-IR (MIR_ON, MIR_OFF pair);

741 (10) XMIR: Approximate MIR (XMIR_ON, XMIR_OFF pair);

742 (11)AE: Alternative exon ends (5', 3', or both);

743 (12) XAE: Approximate AE.

744 Notes, X – exact boundary match for SKIP, approximate (simple exon overlap) for
745 XSKIP;

746 An exon skipping event as a pair between an exon containing ('on') splice form and
747 an exon-skipping ('off') splice.

748 **Fig. 4 KEGG analysis of up-and down-regulated genes after TSA treatment**

749 KEGG analysis was performed and the differentially expressed genes were classified
750 into five categories: cell process, environmental information processing, genetic
751 information processing, metabolism, and organismal systems, and the top 50
752 pathways were presented here. (A) Regarding the up-regulated genes, metabolism
753 accounted for the largest proportion among the categories. Furthermore, the plant
754 hormone signal transduction (46 genes), glutathione metabolism (35 genes), and
755 phenylpropanoid biosynthesis pathways (51 genes) showed the most genes (red
756 arrows). The statistics analysis of enrichment pathways showing the lowest q-value of
757 plant hormone signal transduction, carbon metabolism, and phenylpropanoid
758 biosynthesis pathways also indicated the reliable enrichment significance (blue
759 arrows). (B) In the down-regulated genes, plant hormone signal transduction (48
760 genes), photosynthesis (41 genes), and carbon metabolism pathways (39 genes)
761 showed the most genes (red arrows). The statistics analysis of the three enrichment
762 pathways showed their lowest q-value and the reliable significance of enrichment
763 pathways (blue arrows). Statistics of pathway enrichment of DEGs were conducted
764 using RichFactor and *q*-value. Circle size indicates the gene numbers in the different

765 pathways, is the ratio of differentially expressed gene numbers to all gene numbers in
766 this pathway term. A larger size means a greater number of genes. *Q*-value is
767 corrected *p*-value ranging from 0 to 1, and less *q*-value means greater intensiveness.

768 **Fig. 5 Heatmap of the 94 DEGs associated with hormonal pathways after TSA**
769 **treatment**

770 The heatmap of FPKM (fragments per kilobase of transcript per million reads mapped)
771 of 94 DEGs associated with hormone signal transduction in three biological replicates
772 of Mock and TSA treatment ovules. The DEGs were then divided into four groups
773 (a-d) according to the expression profiles in ovules of mock and TSA treatments. a,
774 The genes significantly up-regulated in response to TSA treatment; b, The genes that
775 showed a weak difference with less FPKM values; c, The genes that showed a weak
776 difference with more FPKM values; d, The genes significantly down-regulated in
777 response to TSA treatment. Log10-transformed (FPKM + 1) expression values were
778 used to create the heat map. The red or green colors represent the higher or lower
779 relative abundance of each transcript in each sample.

780 **Fig. 6 Verification of some key genes transcription associated with**
781 **phytohormones in fiber initiation with Q-PCR**

782 The expression profiles of key genes associated with phytohormone pathways were
783 determined in the mock and TSA-treated ovules by RT-qPCR. All the expression
784 levels were normalized to UBQ7, then the gene was expressed as a ratio relative to
785 mock, which was set to a value of 1. Error bar indicated SD (standard deviation) of
786 three biological replicates. Primers are listed in the Supplementary Table 1.

Fig. 7 Phenotypic observation on initiation and elongation of cultured fibrocytes in vitro under different hormones

(A) -2 DPA (days post anthesis) ovules were cultured in BT medium without GA3 or IAA and supplemented with 20 μM ABA for 7 days (top and middle) or 14 days (bottom) *in vitro*, then the ovule surface were observed and captured by Scanning Electron Microscope for 7 days. The pictures on the middle were the magnification of the regions in the top pictures (for ovules cultured at 7 days, Bar=1 mm (intact ovules). Bar=200 μm (magnification), while for 14-day, Bar=2 mm). (B) Effects of different Methyl jasmonate (MeJA) concentrations (0.05, 0.5 μM) on the development of cultured fibers and ovules of ZM24.

Fig. 8 Proposed model of histone mediated-phytohormone pathways and secondary metabolism/energy metabolism-regulating fiber cell initiation and development

In this model, histone deacetylation modifies some genes transcription associated with different phytohormones and metabolism pathways, then, regulating auxin, GA and JA signalings as well as energy metabolism positively. In contrast, ABA signalings, phenylpropanoid and glutathione metabolism negatively mediate fiber cell initiation and development.

Figures

Figure 1 Application of TSA repress fiber cell initiation and elongation *in vitro*

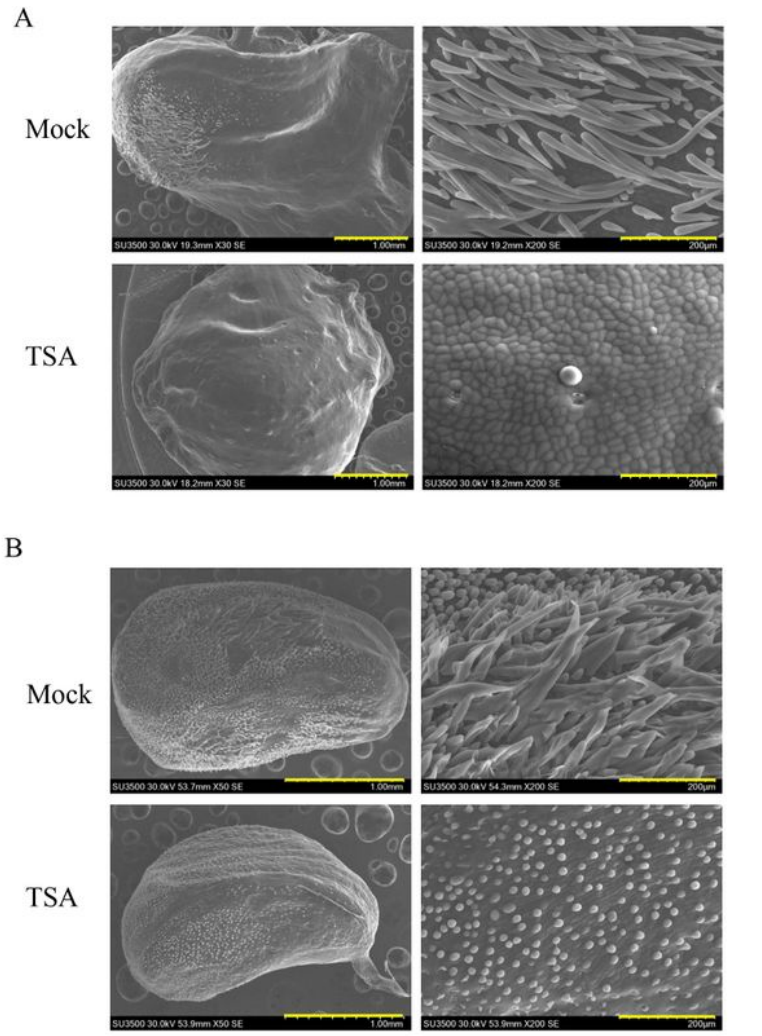

(A) -2 DPA (days post anthesis) ovules were treated with 10 u M TSA for 6 days *in vitro*, then the ovule surface were observed and capture by Scanning Electron Microscope. (B) 0 DPA ovules were treated with 10 μM TSA for 2 days *in vitro*, and the ovule surface were observed and capture by SEM. Bar= 1 mm (intact ovules) and Bar=200 μm (magnification). The pictures on the right was the magnification of the regions in left pictures.

Figure 1

Please See image above for figure legend.

Figure 2 Reads distribution in genome and natural species distribution of identified genes

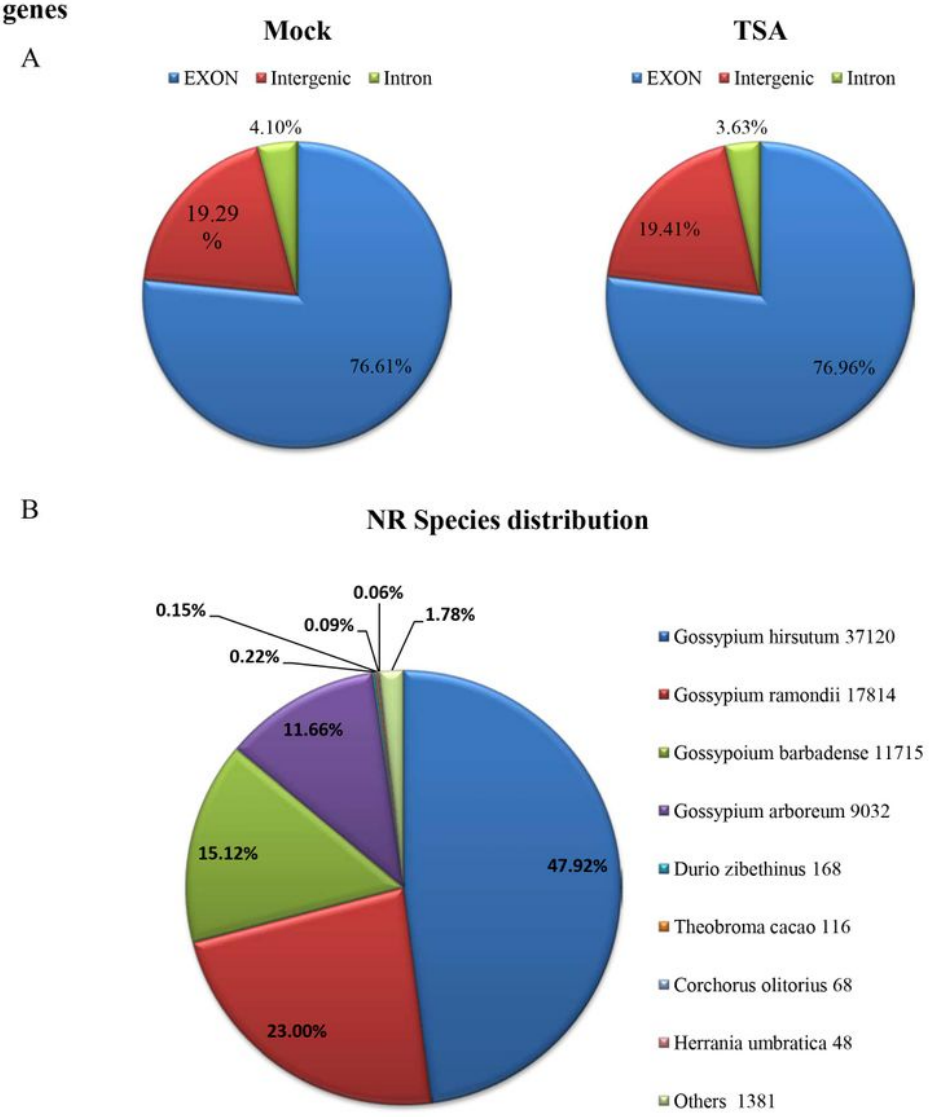

(A) All the reads obtained were mapped to the cotton genome and distribution in exon, intergenic and intron regions was represented for ovules treatment with mock and TSA.
(B) A total of 77,555 unigenes were annotated to the Nr protein database. For the species distribution, about 31,720 (47.92%), 17,814(23%), 11,715 (15.12%) and 9030 (11.66%) unigenes were mathched with *Gossypium hirsutum*, *G. ramondii, G. barbadense* and *G. arboretum*.The matched genes are less than 2% in other close species (i.e. *Durio zibethinus*, *Theobroma cacao*, *Corchorus olitorius*, *Herrania umbratica*).

Figure 2

Please See image above for figure legend.

Figure 3 Alternative splicing analysis of transcripts identified in Mock and TSA treated ovules

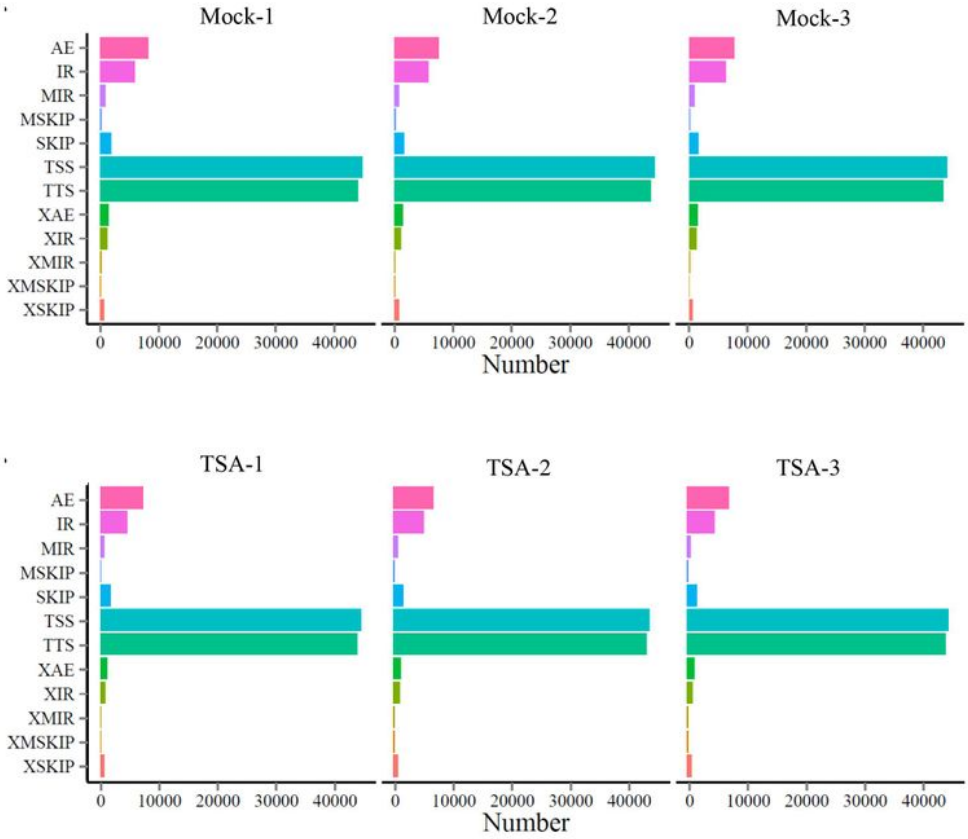

In the six libraries including mock and TSA treated , alternative splicing of the transcripts was analyzed. In total, 12 kinds of AS events were defined as follows, and the results showed that TSS and TSS are the dominant AS events identified.

(1) TSS: Alternative 5‘ first exon (transcription start site) ;
(2) TTS: Alternative 3' last exon (transcription terminal site);
(3) SKIP: Skipped exon(SKIP_ON,SKIP_OFF pair);
(4) XSKIP: Approximate SKIP (XSKIP_ON,XSKIP_OFF pair) ;
(5) MSKIP: Multi-exon SKIP (MSKIP_ON,MSKIP_OFF pair);
(6) XMSKIP: Approximate MSKIP (XMSKIP_ON,XMSKIP_OFF pair);
(7) IR: Intron retention (IR_ON, IR_OFF pair);
(8) XIR: Approximate IR (XIR_ON,XIR_OFF pair);
(9) MIR: Multi-IR (MIR_ON, MIR_OFF pair);
(10) XMIR: Approximate MIR (XMIR_ON, XMIR_OFF pair);
(11)AE: Alternative exon ends (5‘, 3’, or both);
(12) XAE: Approximate AE .

Notes, X – exact boundary match for SKIP, approximate (simple exon overlap) for XSKIP; an exon skipping event as a pair between an exon containing (‘on’) splice form and an exon skipping (‘off’) splice

Figure 3

Please See image above for figure legend.

Figure 4 KEGG analysis of up- and down-regulated genes after TSA treatment

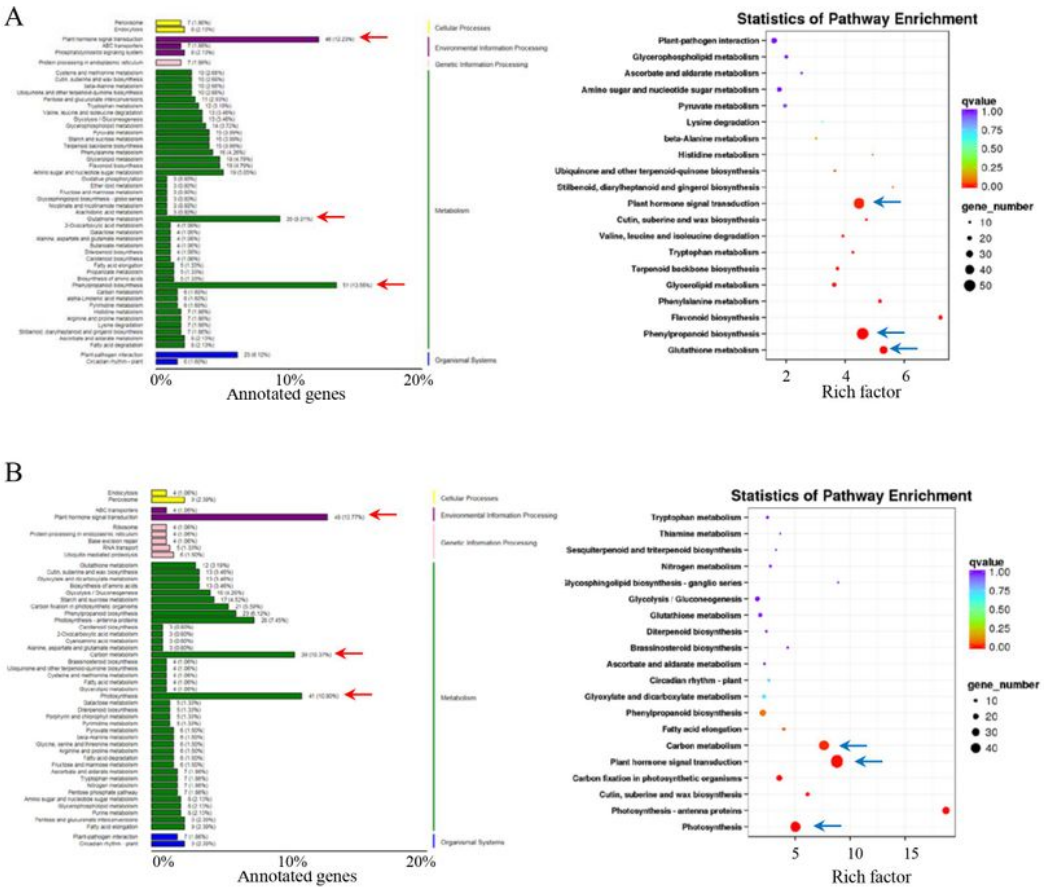

KEGG analysis was performed and the differentially expressed genes were classified into five categories: cell process, environmental information processing, genetic information processing, metabolism and organismal systems, and the top 50 pathways were presented here. (A) Regarding the up-regulated genes, metabolism accounted for the largest proportion among the categories. Furthermore, the plant hormone signal transduction (46 genes), glutathione metaoblism (35 genes) and phenylpropanoid biosynthesis pathways (51 genes) showed the most genes (red arrows). The statistics analysis of enrichment pathways showing the lowest q-value of plant hormone signal transduction, carbon metaoblism and phenylpropanoid biosynthesis pathways also indicated the reliable enrichment significance (blue arrows). (B) In the down-regulated genes, plant hormone signal transduction (48 genes), photosynthesis (41 genes) and carbon metabolism pathways (39 genes) showed the most genes (red arrows). The statistics analysis of the three enrichment pathways showed their lowest q-value and the reliable significance of enrichment pathways (blue arrows). Statistics of pathway enrichment of DEGs were conducted using RichFactor and *q*-value. Circle size indicates the gene numbers in different pathway, is the ratio of differentially expressed gene number to all gene number in this pathway term. Larger size means greater number genes. *Q*-value is corrected *p*-value ranging from 0 to 1, and less *q*-value means greater intensiveness.

Figure 4

Please See image above for figure legend.

Figure 5 Heatmap of the 94 DEGs associated with hormonal pathways after TSA treatment

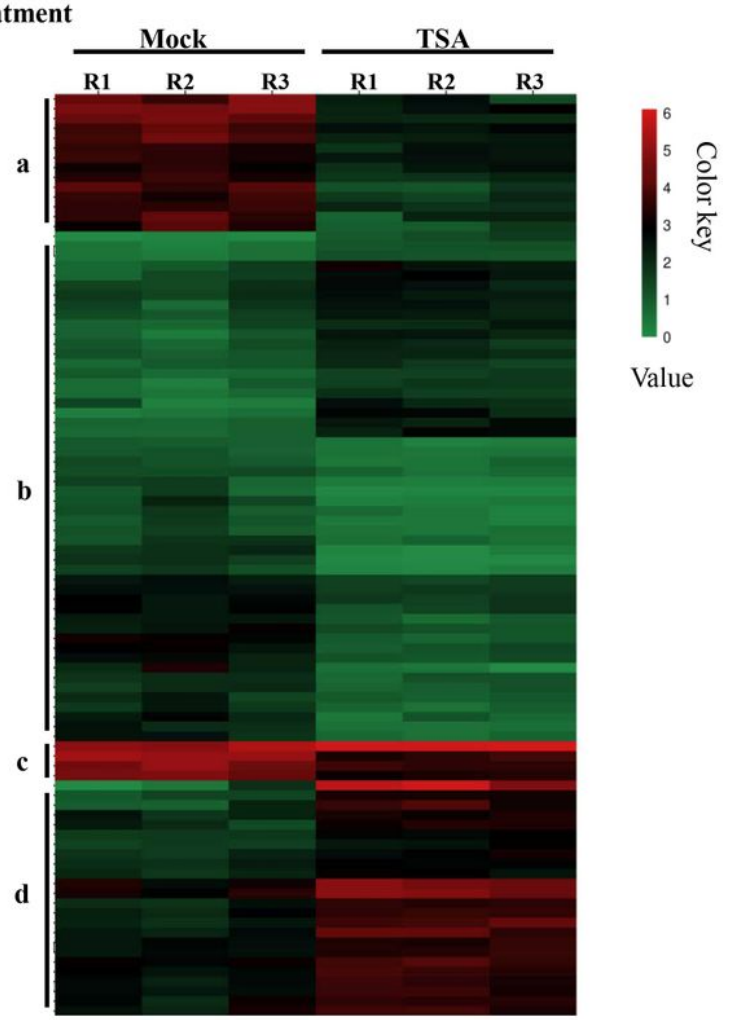

The heatmap of FPKM (fragments per kilobase of transcript per million reads mapped) of 94 DEGs associated with hormone signal transduction in three biological replicates of Mock and TSA treatment ovules. The DEGs were then divided into four group according to the expression profiles in ovules of mock and TSA treatments. **a** The genes significantly up-regulated in response to TSA treatment; **b** The genes that showed a weak difference with less FPKM values; **c** The genes that showed a weak difference with more FPKM values; **d** The genes significantly down-regulated in response to TSA treatment. Log10-transformed (FPKM + 1) expression values were used to create the heat map. The red or green colors represent the higher or lower relative abundance of each transcript in each sample.

Figure 5

Please See image above for figure legend.

Figure 6 Verification of some key genes transcription associated with phytohormones in fiber initiation with Q-PCR

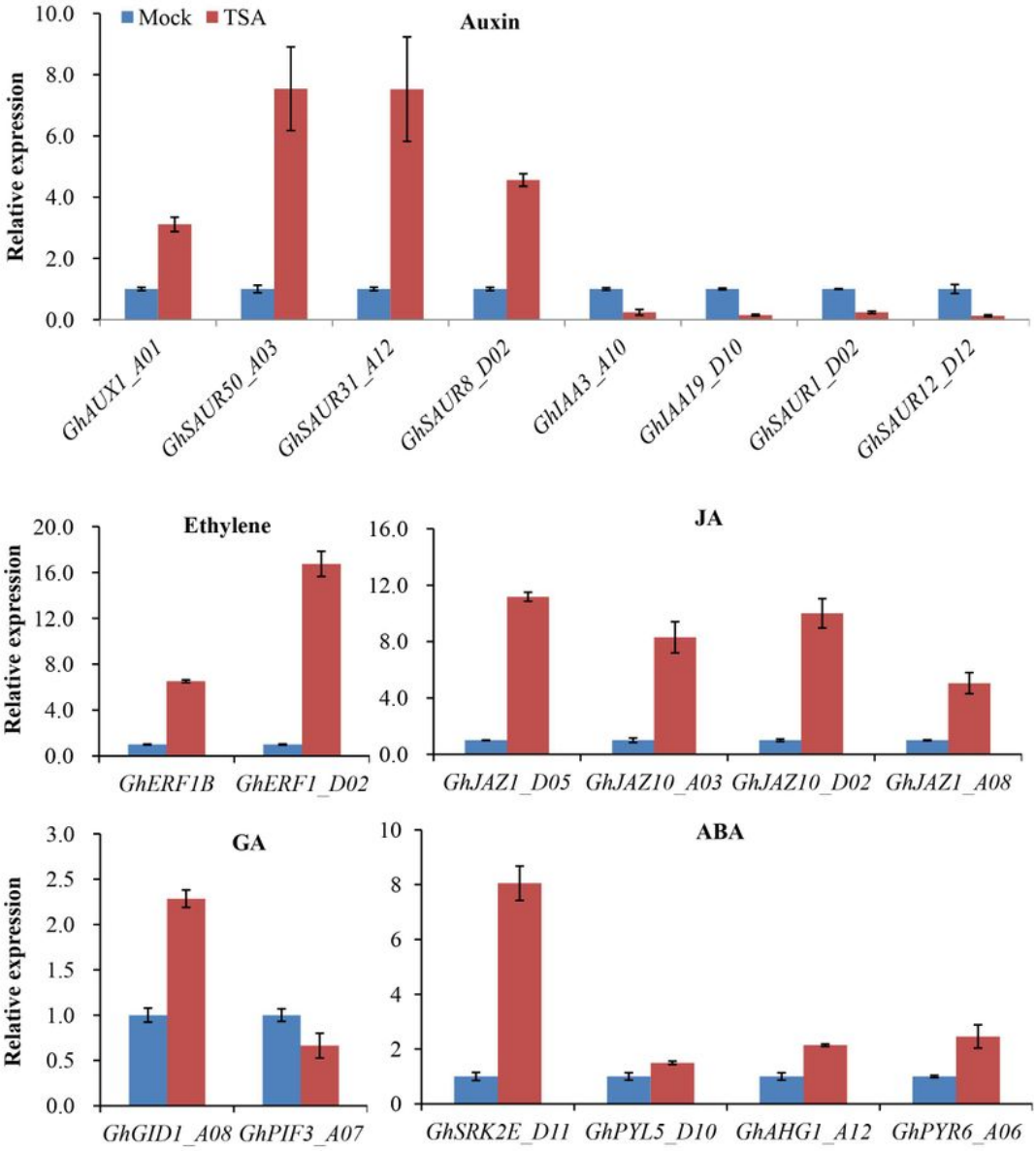

The expression profiles of key genes associated with phytohormone pathway were determined in the mock and TSA treated ovules by RT-QPCR. All the expression levels were normalized to UBQ7, then the gene was expressed as a ratio relative to mock, which was set to a value of 1. Error bar indicated SD (standard deviation) of three biological replicates. Primers are listed in the Supplementary Table 1.

Figure 6

Please See image above for figure legend.

Fig. 7 Phenotypic observation on initiation and elongation of cultured fibrocytes in vitro under different hormones

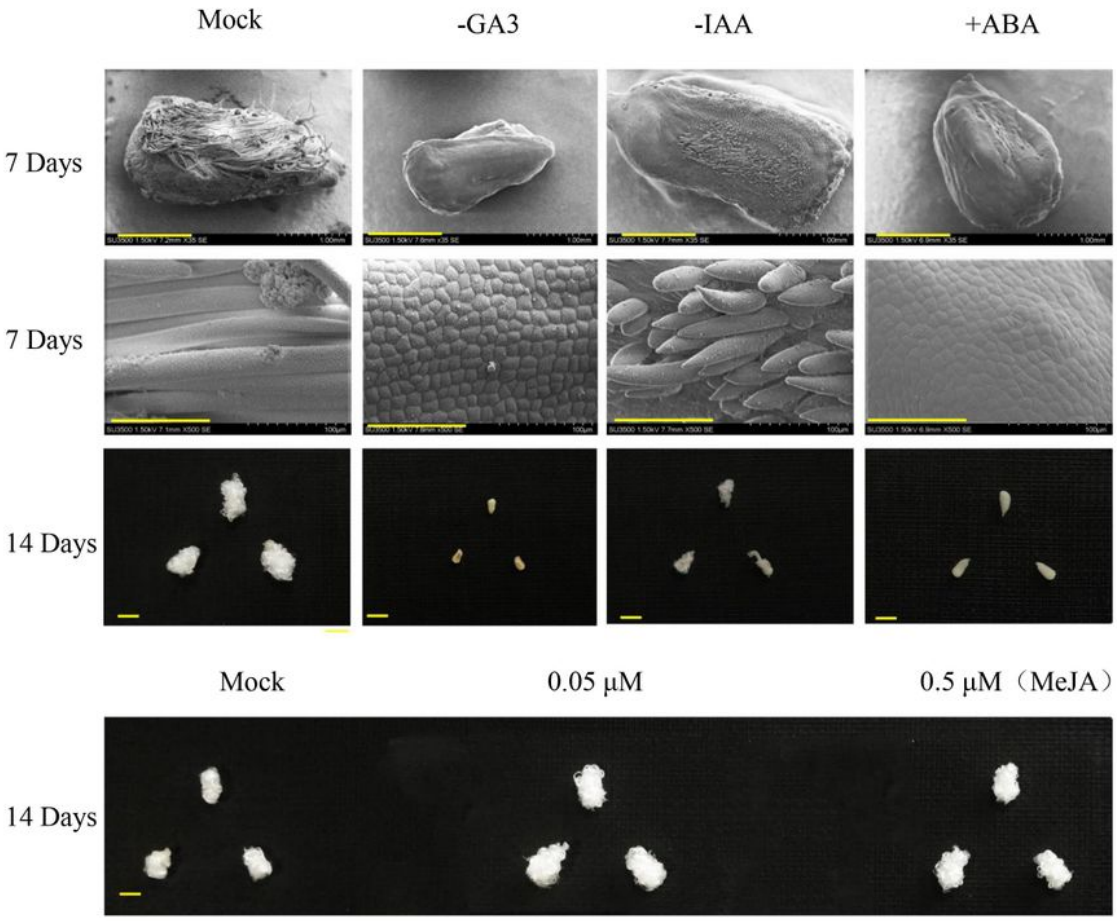

(A)-2 DPA (days post anthesis) ovules were cultured in BT medium without GA3 or IAA and supplemented with 20 μM ABA for 7 days (top and middle) or 14 days (bottom) *in vitro*, then the ovule surface were observed and captured by Scanning Electron Microscope for 7 days. The pictures on the middle were the magnification of the regions in the top pictures (for ovules cultured at 7 days, Bar=1 mm (intact ovules). Bar=200 μm (magnification), while for 14-day, Bar=2 mm). (B) Effects of different Methyl jasmonate (MeJA) concentrations (0.05, 0.5 μM) on the development of cultured fibers and ovules of ZM24.

Figure 7

Please See image above for figure legend.

Figure 8 Proposed model of histone mediated-phytohormone pathways and secondary metabolism/energy metabolism regulating fiber cell initiation and development

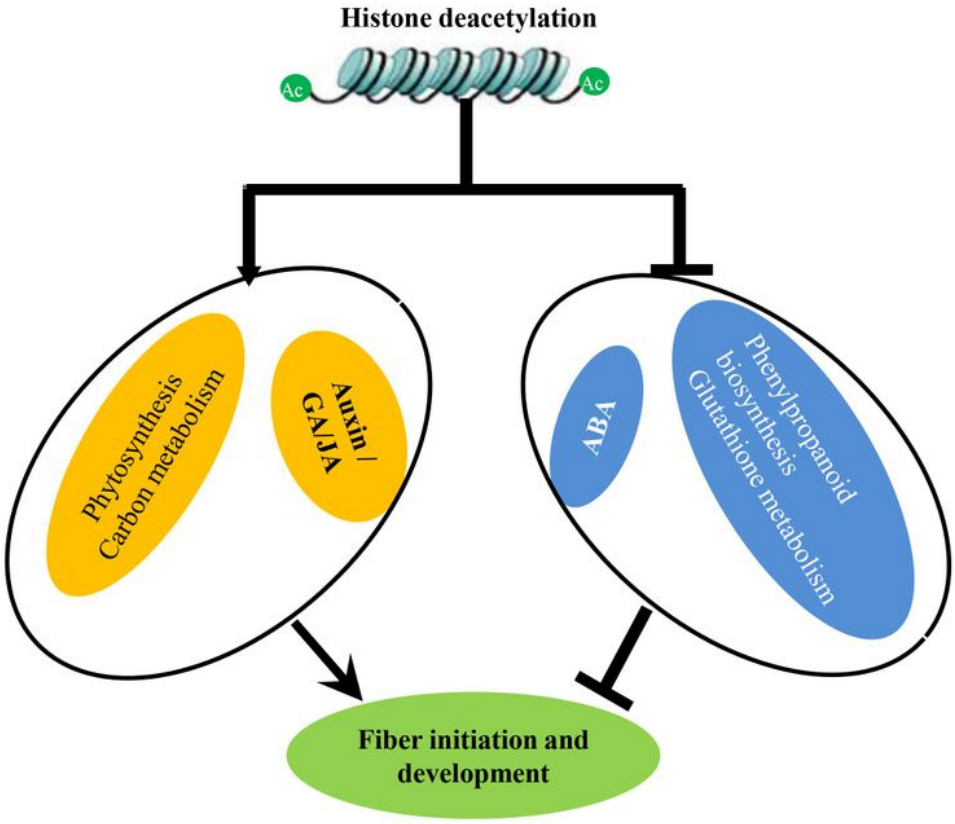

In this model, histone deacetylation modifies some genes transcription associated with different phytohormones and metabolism pathways, then, regulating auxin, GA and JA signalings as well as energy metabolism positively. In contrast, ABA signalings, phenylpropanoid and glutathione metabolism negatively mediate fiber cell initiation and development. .

Figure 8

Please See image above for figure legend.

Supplementary Files

This is a list of supplementary files associated with this preprint. Click to download.

- Supplementalfigures.pdf
- TableS1QPCRprimersusedinthiswork.docx
- TableS2DEGsinmockvsTSA.xls
- TableS3DEGsinhormonesignalingtransduction.xls
- TableS4DEGsrelatedwithhormonesignalinginfourclasses.xls